Colloids and Surfaces B: Biointerfaces 209 (2022) 112212

Contents lists available at ScienceDirect

Colloids and Surfaces B: Biointerfaces

journal homepage: www.elsevier.com/locate/colsurfb

Effect of drag-reducing polymer on blood flow in microchannels

Guanjie Li [a], Yang Sun [a], Xu Zheng [b,*], Hyoung Jin Choi [c], Ke Zhang [a,*]

[a] MIIT Key Laboratory of Critical Materials Technology for New Energy Conversion and Storage, School of Chemistry and Chemical Engineering, Harbin Institute of Technology, Harbin 150001, China

[b] State Key Laboratory of Nonlinear Mechanics, Institute of Mechanics, Chinese Academy of Sciences, Beijing 100190, China

[c] Department of Polymer Science and Engineering, Inha University, Incheon 22212, South Korea

ARTICLE INFO

Keywords:
Hyaluronic acid
Red blood cell
Velocity
Cell-free layer
Microcirculation

ABSTRACT

Drag-reducing polymers (DRPs) can significantly improve blood circulation when added to blood at a nanomolar concentration, manifesting great potential for application in the biomedical field. In this work, hyaluronic acid (HA) was selected as a natural DRP, and its effects on blood microcirculation at different concentrations, flow rates, and channel geometry were studied in microchannels. The experimental results show that adding a small dose of HA can increase the velocity and shorten the thickness of the cell-free layer (CFL or cell depletion layer (CDL)) near the wall. After considering efficiency, our experiments determined 50 ppm addition of HA to be the most suitable amount for improving blood circulation. Our results demonstrate that HA has high efficiency in improving the circulation of blood flow and shed light on unveiling the mechanism of using natural DRPs to cure some cardiovascular diseases.

1. Introduction

Adding a tiny amount of flexible long-chain polymers into a fluid at a small dose can significantly increase the flow velocity of the fluid; this hydrodynamic phenomenon is called the Toms effect. The drag reduction (DR) efficiency of polymers is known to be related to their molecular weight [1,2], chain flexibility [3], polymer concentration [4], salt content (in the case of polyelectrolytes) [5] and other physical and chemical properties [6–9]. High-efficiency friction reduction of DRPs [10] has enabled practical applications in various areas, including industrial hydraulic transportation [11,12] and biomedical fields, such as for tissue perfusion and blood fluid flow in animals [13,14].

The hydrodynamic and rheological properties of the blood circulation system have been found to be closely related to various cardiovascular and cerebrovascular diseases, such as haemorrhagic shock, thrombosis, and coronary ischaemia. In recent years, some animal experiments have shown that DRPs demonstrate surprisingly good effects on the prevention of thrombosis, treatment of haemorrhagic shock and coronary ischaemia. Cotoia et al. [15] reported that low-dose hyaluronic acid (HA) improved the survival rate of rats with haemorrhagic shock. High-molecular-weight polyethylene oxide (PEO) was also found to increase blood velocity and functional capillary density and prolong the survival time of rats with haemorrhagic shock [16]. Hu et al. [17] studied the effect of PEO on ischaemic/reperfusion (I/R) injury of rat hearts, showing that adding PEO could improve coronary blood flow and reduce the activities of lactate dehydrogenase and creatine kinase. Furthermore, Tohme et al. [18] demonstrated that PEO also has an effect on the prevention of liver I/R injury.

The fact that a small amount of DRPs can significantly improve systemic blood circulation has attracted intensive attention from the medical field as well as other interdisciplinary fields. Experiments have been performed to unveil how these factors influence blood flow, and particle tracking velocimetry (PTV) has been used to measure the particle-fluid flow velocity and wall shear stress distribution [19–21]. The effect of DRPs on the thickness of the cell-free layer (CFL) is a notable rheological phenomenon. Although it has been studied widely, the mechanism still cannot be explained clearly. It has been suggested for many years that the factors affecting the thickness of the CFL mainly include the haematocrit of red blood cells (RBCs), diameter of blood vasculature, deformability of RBCs, erythrocyte aggregation, calyx layer, and blood flow rate [22–27]. The CFL thickness was analysed using a high-speed camera to take pictures of RBC suspensions to measure the distance from the suspension to the wall [28,29]. Brands et al. [30] adapted this method to measure the CFL along with the length of a segment of an artery without the use of a high-speed camera, finding that the CFL is not constant in the same location. Kumar and Graham

* Corresponding authors.
E-mail addresses: zhengxu@lnm.imech.ac.cn (X. Zheng), zhangke@hit.edu.cn (K. Zhang).

https://doi.org/10.1016/j.colsurfb.2021.112212

Available online 12 November 2021
0927-7765/© 2022 Elsevier B.V. All rights reserved.

[31] used mathematical models to describe the phenomenon that platelets and leucocytes are close to the wall, in contrast to RBCs.

Although DRPs have shown significant improvement of blood circulation, the current research is mostly limited to animal experiments. The fundamental research is still not systematic, and the mechanism remains unclear. Recently, some studies have investigated the flowing characteristics of RBCs induced by DRPs in a microchannel. Wu et al. [32] found that adding PEO made a significant reduction in CFL thickness and caused a substantial elongation in RBC shape. Bragin [33] showed that adding PEO can make more RBCs enter capillaries and enhance capillary perfusion.

Currently, research on the medicinal value of DRP in curing cardiovascular diseases is generally concentrated on artificial DRPs (such as PEO), and research on natural polymers is rare. Note that natural polymeric HA (extracted from animal tissues or produced from microbial fermentation) is a linear macromolecular (10^5-10^7 Da) mucopolysaccharide composed of the units D-glucuronic acid and N-acetylglucosamine. In this study, HA was selected, and its effect on the viscosity, velocity profile, and CFL of RBC suspensions was systematically studied.

2. Experimental details

2.1. Materials

Anticoagulant horse blood was supplied by Guangzhou Hongquan Biological Technology Company Limited, China. The horse RBC has a biconcave shape and lacks a nucleus, as with the human RBC. (As the horse is a mammal, its RBCs have similarities to those of other mammals not only in shape but also in nature.) In addition, the size of human RBCs usually falls within a range of 6–8 μm. The diameter of horse RBCs (~6 μm) is similar to that of humans. Moreover, the effects of drag reducers on the flows of other mammalian bloods (such as bovine blood [23,30], porcine blood [34], and rat blood [35]) were also studied. HA with a molecular weight of 2000 kDa (HA-2000) was purchased from Xi'an Xaseason Biotechnology Company Limited. Phosphate buffered saline (PBS) was obtained from Harbin Summus Biotechnology Company Limited. Anhydrous ethyl alcohol was supplied by Tianjin Tianli Chemical Reagent Company Limited. Polystyrene and TWEEN-20 were obtained from Duke Scientific Corporation and Ameresco Scientific Corporation, respectively. A polydimethylsiloxane (PDMS) microchannel (straight channel, Fig. 1a) with a rectangular cross-section, as well as a T-type channel (Fig. 1b) with a contraction ratio of $w_1/w_2 = 1/2$ (Fig. 1) were used in experiments. The dimensions of the main channel and daughter branch were 4 mm (length) × 300 μm (width) × 30 μm (height) and 2 mm (length) × 150 μm (width) × 30 μm (height), respectively. w_1 and w_2 stand for the width of the daughter branch and the main channel, respectively. $w_1 = 150$ μm, and $w_2 = 300$ μm. Fig. S1 shows the optical microscope image of the T-type channel under a 20x objective.

2.2. Preparation of reagents

2.2.1. Preparation of RBC suspension

First, 3 mL of horse blood was added into the same volume of PBS for mixing. Subsequently, the mixed reagents were placed in a centrifuge to remove the plasma and buffy coat at 3000 r/min, and the lowest suspension was kept after washing three times. This method is commonly used to get the RBC suspension from the whole blood, which has been reported in many academic literatures [36, 37]. Finally, PBS was added to the washed RBCs to make the haematocrit reach 10%. A haematocrit of 10% was chosen because of the existence of the Fåhraeus phenomenon associated with the microcirculatory haematocrit in vivo, which is less than the systemic haematocrit [38,39].

2.2.2. Preparation of HA stock solution

First, 0.01 g HA was dissolved in 20 mL of water with stirring via a glass rod to form a well-mixed solution. Second, the solution was transferred into a sealed beaker for 24 h and then mixed by a magnetic stirrer at a low mixing speed for an hour. Finally, the mother liquor of HA was obtained after filtration.

2.3. Characterisation of RBC suspension

RBC flow behaviour was observed by a microscopic flow imaging system that consisted of a fluorescent inverted microscope (IX 71, Olympus, Japan), an EMCCD camera (ixon DV897, Andor, British), a syringe pump (CN-74900-45, Cole-Parmer, USA), and a PC (Fig. 2). In

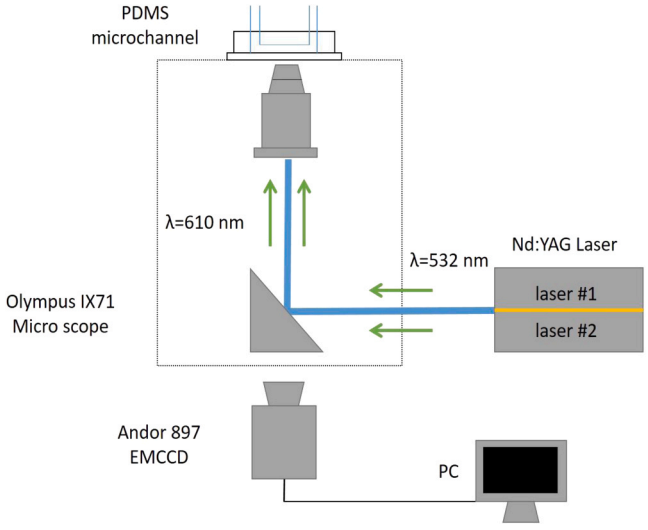

Fig. 2. Schematic of the micro flow imaging system.

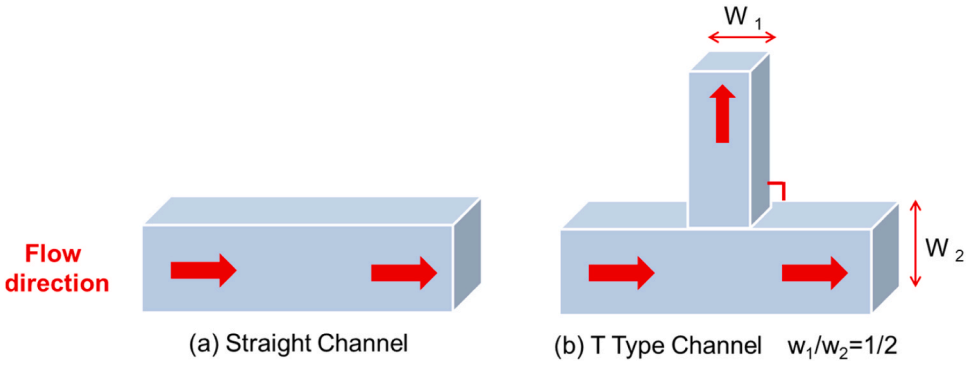

Fig. 1. PDMS microchannels with different geometries. (a) Straight Channel. (b) T type Channel.

the PTV measurement, the size of fluorescent tracer particles (American Duke Technology Company) is 1 μm. Each point of the measured velocity profile represents the average velocity calculated from all the tracking results in an interrogation area with a width of about 5–10 μm, corresponding to 32–64 pixels (image resolution is 0.16 μm/pixel). The size of the tracer particles is only approximately 17% that of the RBC (approximately 6 μm) in the present experiment. A rheometer (MCR 502, Anton Paar, Austria) was used to test the viscosity of the RBC suspension with different concentrations of HA at 25 °C. The velocity field distribution of blood in the microchannel was obtained by PTV. The thickness of the CFL was measured from the figures, in which the CFL can be visualised by overlapping all frames using the Z Project method from ImageJ software.

The nominal wall shear rate in the system was calculated using Eq. (1) [40],

$$\dot{\gamma} = \frac{6Q}{wh^2} \tag{1}$$

where Q is the volumetric flow rate, w is the width of the rectangular cross-section, and h is the height of the rectangular cross-section. In the present experiment, the flow rates Q are fixed to be approximately 300 μL/h and 500 μL/h. The corresponding wall shear rates are 1852 s^{-1} and 3086 s^{-1}.

The thickness reduction % (TR%) was calculated using Eq. (2),

$$TR\% \left| \frac{T_1 - T_0}{T_0} \right| \times 100\% \tag{2}$$

where T_0 is the thickness of the CFL in the RBC suspension without a DRP and T_1 is the thickness of the CFL in the RBC suspension with a DRP.

3. Results and discussion

We first clarify the physical regimes of our current study based on the Reynolds number Re and Weissenberg number Wi. The Re number, defined as $Re = \rho uL/\mu$ (where ρ, u, L, and μ are the density of the polymer solution, the typical velocity, the typical dimension of the channel, and the viscosity of the polymer solution, respectively), is estimated to be approximately 0.002 – 0.04. The Wi number, calculated by $Wi = \tau\dot{\gamma}$ (where τ is relaxation time and $\dot{\gamma}$ is wall shear rate), is estimated to be about 185 and 309 at 300 μL/h and 500 μL/h, respectively. Thus, this study is in the low Re and large Wi number regime, where viscous effect dominates over inertial effect, while elastic effect is even much stronger than the viscous effect when we consider the lateral migration of cells near wall.

3.1. Effect of HA on the viscosity of the RBC suspension

Fig. S2(b) shows the shear viscosity of the RBC suspension changing with the shear rate, following the addition of 0, 10, 20, 50 and 80 ppm HA with a molecular weight of 2000 kDa to the RBC suspension. A decrease in all the viscosities was found with increasing shear rate, demonstrating that the RBC suspension is a non-Newtonian liquid with a shear-thinning property at a low-shear-rate range. Some studies have found that the aggregation of RBCs causes an increase in viscosity at a low-shear-rate region [41]. Similar RBC orientations may promote the formation of RBC stacks at low shear rates that increase the viscosity. Furthermore, it can also be noted that all the suspensions with different HA concentrations behave as a Newtonian fluid, and these viscosity curves overlap when the shear rate > 500 s^{-1}, which is also reported by Marhefka et al. [14]. At a higher shear rate, the individualisation, alignment, and stretching of RBCs reduce the viscosity [42,43]. Thus, the addition of HA barely influences the RBC viscosity at the shear rates, HA concentrations, and haematocrit used in our study (Fig. S2(b)).

3.2. Effect of HA on the velocity profile of the RBC suspension

A PTV technique was applied to obtain the velocity field of the RBC suspension. A syringe pump was used to induce RBC suspension flow through the microchannel. The velocity field data were calculated by the PTV with the images of the flowing RBC suspension taken by a high-speed camera. Fig. 3 shows the experimental velocity field measured at a horizontal plane at approximately z ~ 1 μm, close to the substrate in the experimental channel calculated by PTV. Theoretically, the velocity profile $u_x(y,z)$ in such a channel with a rectangular cross-section can be expressed as (see Supporting Information for details):

$$u_x\left(y,z\right) = \frac{4h^2\Delta p}{\pi^3\mu L}\sum_{n=1,3,5.}^{\infty}\frac{1}{n^3}\left[1-\frac{\cosh(n\pi y/h)}{\cosh(n\pi w/2h)}\right]\sin\left(n\pi z \Big/ h\right) \tag{3}$$

where w and h are respectively the width and height of the rectangular cross-section; the axes y and z are along the width and height directions, respectively; μ is viscosity; and $\Delta p/L$ is the pressure gradient. As the flow rate Q was controlled in the experiment, Eq. (3) can also be written as:

$$u_x\left(y,z\right) = \frac{48Q}{\pi^3 hw}\frac{\sum_{n=1,3,5.}^{\infty}\frac{1}{n^3}\left[1-\frac{\cosh(n\pi y/h)}{\cosh(n\pi w/2h)}\right]\sin\left(n\pi z \Big/ h\right)}{\left[1-\sum_{n=1,3,5.}^{\infty}\frac{1}{n^5}\frac{192}{\pi^5}\frac{h}{w}\tanh\left(n\pi w \Big/ 2h\right)\right]} \tag{4}$$

By comparing the experimental velocity with Eq. (4), we find that the experimental velocities close to the substrate (Fig. 3a and b) are in agreement with the theoretical values given the fixed flow rate at Q = 300 μL/h and 500 μL/h, respectively, with an average value of approximately 0.5 mm/s. As the width (w = 300 μm) of the channel is much larger than the height (w = 30 μm), we can see that the horizontal velocity profile along the width direction appears very flat in the middle, which is consistent with the theoretical profile calculated from Eq. (4) (the 3D theoretical profile is given in the Fig. S4).

The velocity in the middle of the microchannel was the fastest, while it became the slowest near the wall. The velocity of the RBC suspension increased when HA was added under both velocity conditions. The velocity of 50 ppm HA addition was similar to that of 80 ppm HA addition, especially at a higher wall shear rate. The motion of RBCs in the microchannel was not a simple rigid motion but one that exhibits deformation and stretching [44]. The increase in the velocity is considered to be caused by the interaction between RBCs and HA. As a result, the measured velocity profiles with HA manifest microscopic viscosities smaller than the macroscopic nominal values. This effect is expected to change the distribution of the RBCs in the blood flow, indicating that not only the hydrodynamic condition but also the microrheological condition is important. Another issue that influences the velocity profile is the boundary slip, which might be significantly enhanced by DRPs. We plot the experimental velocity profiles near the wall and fit them with Eq. (4) plus a slip boundary condition, as shown in Fig. 3(c). The measured velocity and the fit curve of 0 ppm HA solution indicate a non-slip boundary condition at the side wall. Compared to the measured velocity without adding HA, the near-wall velocity increases obviously with increasing HA concentration. By extrapolating the velocity profile to the wall, we are able to estimate the apparent slip velocity $u_{slip} = 0.03$ mm/s for 20 ppm HA addition and $u_{slip} = 0.04$ mm/s for 80 ppm HA addition, respectively. This value is more than 10% of the average velocity in the same horizontal plane, and thus, it is not negligible. By our method, we are confident in detecting a wall slip velocity larger than 0.02 mm/s. According to the Navier slip model [45], the apparent boundary slip length b is thus $b = u_{slip}/\dot{\gamma} \sim$ 0.02 μm. It is worth noting that the measured viscosity using rheometer increases with the HA concentration as well (Fig. S2 in the Supporting Information). Thus, we suspect that the enhanced near wall flow by adding HA is related to the near wall depletion structure as we will show

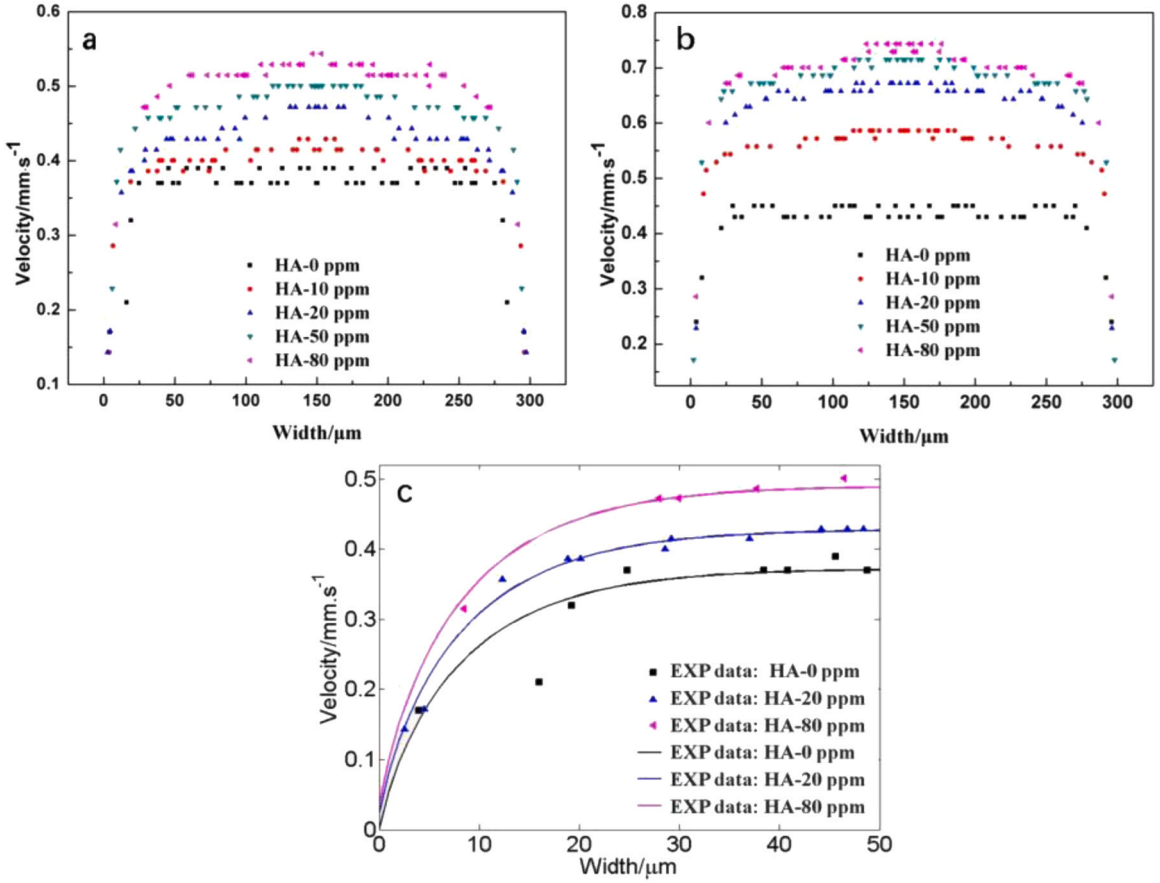

Fig. 3. Comparison of the effect of HA on the velocity profiles of RBC suspensions (10% haematocrit) at different wall shear rates (a) 1852 s^{-1}, (b) 3086 s^{-1}. (c) The near-wall experimental velocity compared with the theoretical fits.

later, and is not directly attributed to the variation of apparent viscosity.

With the development of new technology, the measurement of blood velocity can be achieved via Micro-PIV [34, 46, 47], but there have been few studies on the effect of drag reduction on the flow rate of blood. Fenech et al. [48] studied the effect of sodium alginate on the flow rate of blood. However, in that study, the velocity distribution of a certain cross-section was not given. Only the maximum speed through a certain cross-section was tested. There are not enough data to correlate the effect of the drag reduction with the velocity variation. In contrast, we studied the velocity distribution of blood after adding HA. The results show that the overall velocity distribution improved after adding HA, and we established a relationship between the velocity and HA concentration.

3.3. *Effect of HA on the thickness of the CFL*

We show in this section that HA not only influences the hydrodynamic properties discussed above but also varies the structure of complex blood flow. The most dramatic phenomenon is the variation of the CFL (Fig. 4 and Fig. 5). The thickness of the CFL was measured from the figures, in which the CFL can be visualised by overlapping all frames using the Z Project method from ImageJ software. Fig. 4 shows the effect of HA on the thickness of the CFL in the straight channel. It can be found that the thickness of the CFL near the wall decreases more when HA is added and decreases with decreasing velocity. Furthermore, the thickness of the RBC suspension reaches a minimum when the concentration of HA was 50 ppm. Under the wall shear rate of 1852 s^{-1}, the CFL thickness of the control group without the presence of HA is approximately 2.99 μm, while the CFL thickness is minimised to approximately 1.17 μm after adding 50 ppm HA. At the wall shear rate of 3086 s^{-1}, the

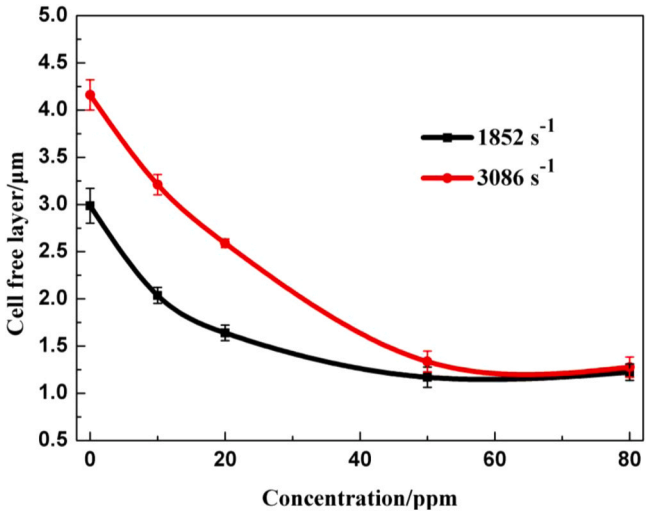

Fig. 4. Comparison of the effect of HA on the thickness of the CFL at different wall shear rates.

CFL thickness of the control group is approximately 4.16 μm, which is reduced to approximately 1.34 μm after adding 50 ppm HA. This proves that HA is effective in reducing the thickness of the CFL. The phenomenon in which RBCs are close to the blood vessel wall can promote oxygen transportation and increase the viscosity near the wall, leading the shear stress of the vessel wall to increase, which then promotes vasodilation [14]. Also, Zhao et al. [49]. found that the concentration of

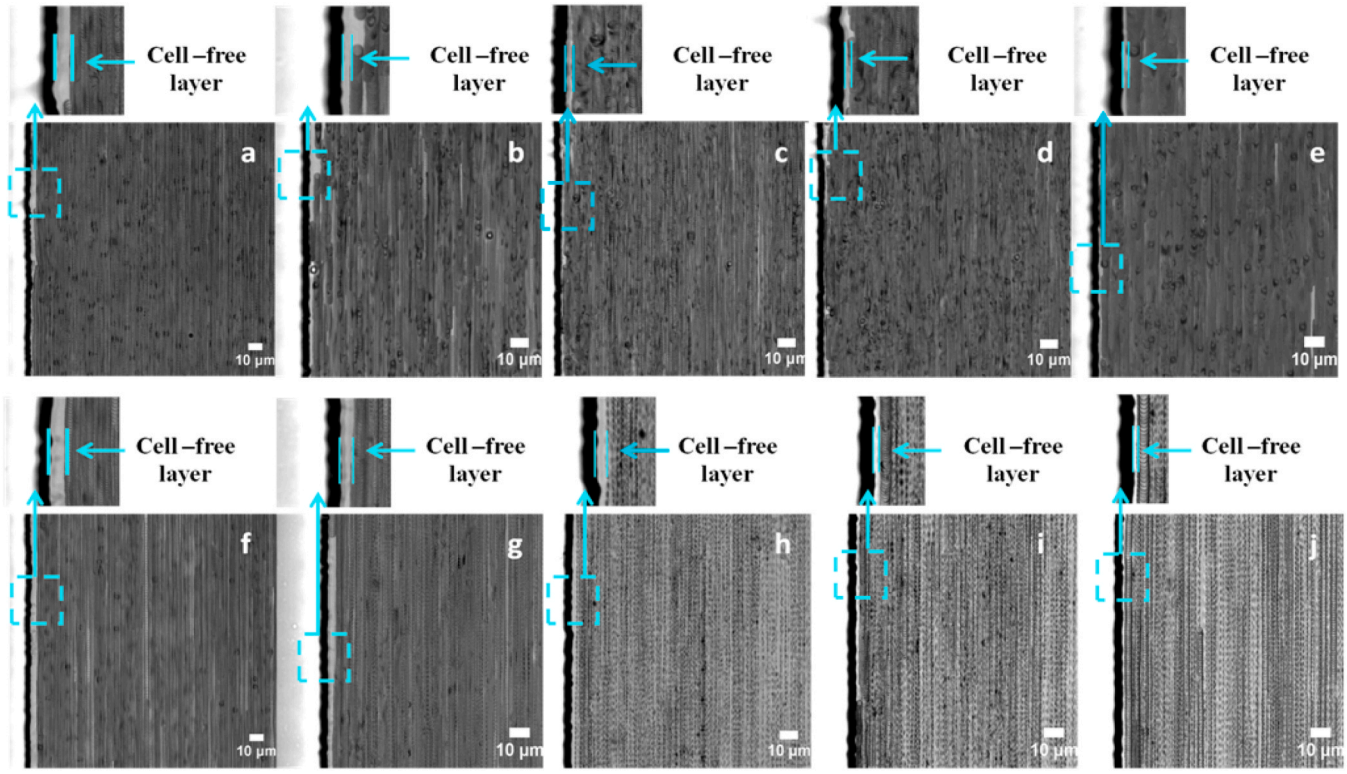

Fig. 5. Effect of HA (10 ppm, b, g; 20 ppm, c, h; 30 ppm, d, i; 50 ppm, e, j) on reducing the CFL thickness near the wall of a straight channel in contrast to the results of control groups (a, f) at different wall shear rates (top, 1852 s^{-1}; bottom, 3086 s^{-1}).

platelet-sized particles near the wall was significantly decreased after adding PEO (10 ppm, the molecular weight of 4500 kDa), indicating the DRPs may be beneficial to intervene near-wall accumulation of platelets and reduce thrombosis. The existing mechanisms on polymer induced turbulent drag reduction are not applicable to explain their effects on hemodynamics because Reynold number of typical blood flow in microvessels ranges from 0.1 to 100. It is not turbulent [14].

Although the generation of the CFL near the wall is still under debate, the possible mechanisms are commonly attributed to both hydrodynamic and rheological properties. Kameneva et al. [50] indicated that the alignment and stretching of polymer molecules might affect the rotation of RBCs, which mainly causes the formation of CFLs. The CFL is also thought to be the result of the axial migration of RBCs, and Secomb et al. [26] proved that the tendency of RBCs flowing away from the vessel wall is caused mainly by the deformability and asymmetry of RBCs. Besides, due to the large value of the Wi number, the elastic normal stress might cause significant lateral migration [51], which is also a considerable mechanism. The axial migration of RBCs is suppressed by cell-cell interactions that push the cells towards the wall; the core of the RBC column has a dispersion effect on cells to push them radially outward [52]. The coupling between the polymer and RBCs enhances the dispersion of cells in the core of the RBC column. Thus, the dispersion drives the cells towards the wall, which counteracts the tendency of the axial migration of RBCs [52]. On the other hand, the decrease of CFL thickness cannot keep decreasing with the increase of HA concentration because of the presence of the elastic normal stress. In our experiment, it is found that the CFL becomes steady at a high concentration of 80 ppm, and the addition of 50 ppm HA is shown to be the most suitable amount required. Based on biocompatibility and turbulent drag-reducing properties, Lim et al. [53] also selected the HA as the additives in their study. With the aid of the micromolar of HA, they effectively manipulated the focal position of particles in a rigid (epoxy-based) microchannel at Reynolds numbers up to Re ≈ 10,000. They also verified that the particle migration in a viscoelastic fluid could be achieved when both elasticity and inertia are present (that is, Wi>>1 and Re>>1). In addition, Leshansky et al. [54] reported that the tuneable viscoelastic focusing of particles could be carried out in the microchannel by adjusting the rheology properties of the carrier solution. There are a large number of branch vessels in the human body. Therefore, we studied the blood flow induced by DRP not only in the straight microchannel but also in the branch vessel (T-type microchannel). In the T-type microchannel, it is convenient for us to observe the variation of flow separation at the bifurcation when DRP is added. Therefore, the effect of HA on the thickness of the CFL at the entrance of the daughter branch was studied in the T-type channel ($w_1/w_2 = 1/2$). The results show that adding HA is very effective for reducing the CFL thickness (Fig. 6). The thickness of the CFL was also measured by overlapping all frames using the Z Project method from ImageJ software. At a wall shear rate of 1852 s^{-1}, the CFL thickness of the control group is approximately 1.1 μm, which is minimised to approximately 0.74 μm after adding 50 ppm HA, and the TR% is 32.7%. Additionally, at a wall shear rate of 3086 s^{-1}, the CFL thickness of the control group is approximately 1.03 μm, which is minimised to approximately 0.64 μm after adding 50 ppm HA, and the TR% reaches 37.9%. This result indicates that adding HA eliminates the flow separation when the RBCs flow through the T-type channel. Similar to the concept of the boundary layer, we know that the decrease of the layer thickness indicates a low mass or momentum loss near the wall by adding DRPs, which is consistent with our observation of faster near-wall flow as shown in Fig. 3(c).

In addition, some researchers have also explored the thickness of the CFL in blood flow under different conditions. Kameneva [14] studied the effect of PEO on the thickness of CFLs with different molecular weights, indicating that polymers with high molecular weights can play a significant role in reducing the thickness of CFLs. However, their CFL thickness data were obtained from only a single-frame image captured by a high-speed camera. The data are inaccurate and require re-evaluation. In addition, there is no concentration effect of PEO on the

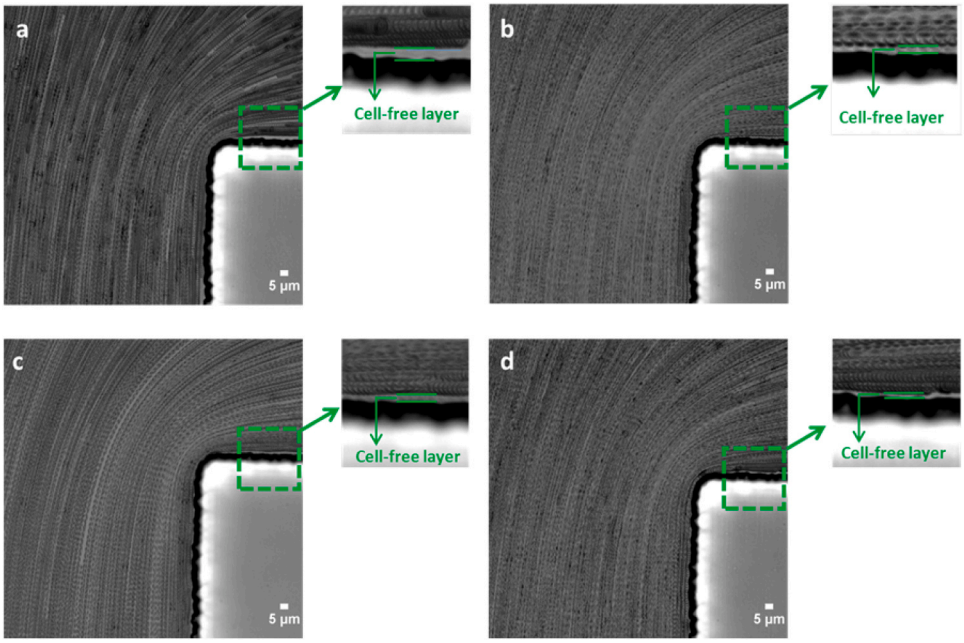

Fig. 6. Effect of HA (50 ppm, c, d) on reducing the CFL thickness at the entrance of the daughter branch in the T-type channel compared to the results of the control group (a, b) at different wall shear rates (a, c 1852 s^{-1}; b, d 3086 s^{-1}).

CFL, and we cannot obtain the regularity conclusion. In contrast, we obtained the CFL thickness data by using a multi-frame superposition. Compared with the single-frame image, the error was significantly smaller. We also established a correlation between the CFL and polymer concentration. Unlike most researchers, who choose synthetic polymers such as PEO, which are commonly used in the industry as drag reducers, we selected HA with its high biocompatibility to be safer from biological perspective. Besides, HA has a negative charge, unlike nonionic polymers such as PEO, and its molecular chain is repelled by the same kind of charge in aqueous solution. HA is more stretched in the blood, and the chance of interaction with RBCs is greater. Also, HA is a semi-rigid polymer, Hong et al. [5] reported that more rigid polymeric chain produces more DR efficiency based on the experimental results from the salt effect on DR of xanthan gum.

4. Conclusions

A systematic study on how natural DRP HA can improve blood circulation in microchannels was conducted, in which the effect of the addition of HA on the viscosity, velocity, and CFL thickness of RBC suspension was investigated. In this study, a significant enhancement of the blood velocity in the microchannel using HA was experimentally verified. Additionally, the CFL thickness in a straight channel is reduced by over 60% with the most suitable addition of 50 ppm HA, and the CFL thickness in the T-type channel is reduced by over 30% with 50 ppm HA, indicating that HA can eliminate the flow separation at the entrance of the daughter branch. These observations point to the conclusion that as a natural DRP, HA has a significant effect on improving blood microcirculation by increasing flow velocity and reducing CFL thickness. These findings also provide novel insight into the application of natural DRPs in the field of curing coronary ischaemic disease, haemorrhagic shock, and thrombus.

CRediT authorship contribution statement

Guanjie Li: Conceptualization, Methodology, Formal analysis, Investigation, Writing – original draft, Visualization. **Yang Sun**: Validation, Formal analysis. **Xu Zheng**: Methodology, Formal analysis, Resources, Writing – original draft. **Hyoung Jin Choi**: Writing – review & editing. **Ke Zhang**: Conceptualization, Formal analysis, Resources, Writing – review & editing, Supervision.

Declaration of Competing Interest

The authors declare that they have no known competing financial interests or personal relationships that could have appeared to influence the work reported in this paper.

Acknowledgements

This work is supported by the National Natural Science Foundation of China (No. 51603056, 11572335), the Excellent Youth Foundation of Heilongjiang Province of China (YQ2019E020), the CAS Key Research Program of Frontier Sciences (QYZDB-SSW-JSC036), and the CAS Strategic Priority Research Program (XDB22040403).

Appendix A. Supporting information

Supplementary data associated with this article can be found in the online version at doi:10.1016/j.colsurfb.2021.112212.

References

[1] L.C. Edomwonyi-Otu, P. Angeli, Separated oil-water flows with drag reducing polymers, Exp. Therm. Fluid Sci. 102 (2019) 467–478.
[2] K. Zhang, G.H. Lim, H.J. Choi, Mechanical degradation of water-soluble acrylamide copolymer under a turbulent flow: effect of molecular weight and temperature, J. Ind. Eng. Chem. 33 (2016) 156–161.
[3] G.H. Lim, H.J. Choi, F. Renou, A.N. Roy, Effects of hydrophobic modification of xanthan gum on its turbulent drag reduction characteristics, J. Ind. Eng. Chem. 54 (2017) 146–150.
[4] H.A. Abdulbari, A. Shabirin, H.N. Abdurrahman, Bio-polymers for improving liquid flow in pipelines—a review and future work opportunities, J. Ind. Eng. Chem. 20 (2014) 1157–1170.
[5] C.H. Hong, H.J. Choi, K. Zhang, F. Renou, M. Grisel, Effect of salt on turbulent drag reduction of xanthan gum, Carbohydr. Polym. 121 (2015) 342–347.
[6] R. Hidema, H. Suzuki, S. Hisamatsu, Y. Komoda, Characteristic scales of two-dimensional turbulence in polymer solutions, AIChE J. 60 (2014) 1854–1862.
[7] A.M. Shetty, M.J. Solomon, Aggregation in dilute solutions of high molar mass poly (ethylene) oxide and its effect on polymer turbulent drag reduction, Polymer 50 (2009) 261–270.

[8] S. Suksamranchit, A. Sirivat, A.M. Jamieson, Polymer-surfactant complex formation and its effect on turbulent wall shear stress, J. Colloid Interface Sci. 294 (2006) 212–221.
[9] A.N.T. Tiong, P. Kumar, A. Saptoro, Reviews on drag reducing polymers, Korean J. Chem. Eng. 32 (2015) 1455–1476.
[10] E.J. Soares, R.N. Siqueira, L. Leal, K.C.O. Barbosa, D.F. Cipriano, J.C.C. Freitas, The role played by the aging of Aloe vera on its drag reduction properties in turbulent flows, J. Non-Newton. Fluid Mech. 265 (2019) 1–10.
[11] M.A. Asidin, E. Suali, T. Jusnukin, F.A. Lahin, Review on the applications and developments of drag reducing polymer in turbulent pipe flow, Chin. J. Chem. Eng. 27 (2019) 1921–1932.
[12] V. Guersoni, A.C. Bannwart, T. Destefani, E. Sabadini, Comparative study of drag reducers for light hydrocarbon flow, Pet. Sci. Technol. 33 (2015) 943–951.
[13] H.L. Greene, R.F. Mostardi, R.F. Nokes, Effects of drag reducing polymers on initiation of atherosclerosis, Polym. Eng. Sci. 20 (1980) 499–504.
[14] J.N. Marhefka, R. Zhao, Z.J. Wu, S.S. Velankar, M.V. Kameneva, Drag reducing polymers improve tissue perfusion via modification of the RBC traffic in microvessels, Biorheology 46 (2009) 281–292.
[15] A. Cotoia, M.V. Kameneva, P.J. Marascalco, M.P. Fink, R.L. Delude, Drag-reducing hyaluronic acid increases survival in profoundly hemorrhaged rats, Shock 31 (2009) 258–261.
[16] Z. Zeng, Q. Zhang, Y. Gao, T. Li, X. Dai, Q. Huang, Z. Chen, Drag-reducing polyethylene oxide improves microcirculation after hemorrhagic shock, J. Surg. Res. 202 (2016) 118–125.
[17] F. Hu, Y. Wang, K. Gong, G. Ge, M. Cao, P. Zhao, X. Sun, Z. Zhang, Protective effects of drag-reducing polymers on ischemic reperfusion injury of isolated rat heart, Clin. Hemorheol. Microcirc. 62 (2016) 1–11.
[18] S. Tohme, M.V. Kameneva, H.O. Yazdani, V. Sud, J. Goswami, P. Loughran, H. Huang, R.L. Simmons, A. Tsung, Drag reducing polymers decrease hepatic injury and metastases after liver ischemia-reperfusion, Oncotarget 8 (2017) 59854–59866.
[19] Y. Ichikawa, K. Yamamoto, M. Motosuke, Three-dimensional flow velocity and wall shear stress distribution measurement on a micropillar-arrayed surface using astigmatism PTV to understand the influence of microstructures on the flow field, Microfluid. Nanofluid. 22 (2018) 73.
[20] S.I. Satake, T. Kunugi, K. Sato, T. Ito, J. Taniguchi, Three-dimensional flow tracking in a micro channel with high time resolution using micro digital-holographic particle-tracking velocimetry, Optic. Rev. 12 (2005) 442–444.
[21] N. Sato, J. Yao, M. Sugawara, M. Takei, Numerical study of particle-fluid flow under AC electrokinetics in electrode-multilayered microfluidic device, IEEE Trans. Biomed. Eng. 66 (2018) 453–463.
[22] S. Kim, R.L. Kong, A.S. Popel, M. Intaglietta, P.C. Johnson, Temporal and spatial variations of cell-free layer width in arterioles, Am. J. Physiol. Heart Circ. Physiol. 293 (2007) H1526–H1535.
[23] J.N. Marhefka, P.F. Moon-Massat, G.P. Dube, W.R. Light, D.A. Freilich, A.J. Russell, M.V. Kameneva, Blood soluble polymers for enhancing near-vessel-wall RBC traffic in presence of hemoglobin based oxygen carrier, Int. J. Eng. Sci. 83 (2014) 138–145.
[24] B. Namgung, H. Sakai, S.H. Kim, Influence of erythrocyte aggregation at pathological levels on cell-free marginal layer in a narrow circular tube, Clin. Hemorheol. Microcirc. 61 (2015) 445–457.
[25] A.R. Pries, T.W. Secomb, P. Gaehtgens, The endothelial surface layer, Pflüg. Arch. Eur. J. Physiol. 440 (2000) 653–666.
[26] T.W. Secomb, B. Styp-Rekowska, A.R. Pries, Two-dimensional simulation of red blood cell deformation and lateral migration in microvessels, Ann. Biomed. Eng. 35 (2007) 755–765.
[27] Z. Shen, G. Coupier, B. Kaoui, B. Polack, J. Harting, C. Misbah, T. Podgorski, Inversion of hematocrit partition at microfluidic bifurcations, Microvasc. Res. 105 (2016) 40–46.
[28] S. Kim, R.L. Kong, A.S. Popel, M. Intaglietta, P.C. Johnson, A computer-based method for determination of the cell-free layer width in microcirculation, Microcirculation 13 (2015) 199–207.
[29] P.K. Ong, S. Jain, B. Namgung, Y.I. Woo, H. Sakai, D. Lim, K.J. Chun, S. Kim, An automated method for cell-free layer width determination in small arterioles, Physiol. Meas. 32 (2011) N1–12.
[30] J. Brands, D. Kliner, H.H. Lipowsky, M.V. Kameneva, F.S. Villanueva, J.J. Pacella, New insights into the microvascular mechanisms of drag reducing polymers: effect on the cell-free layer, PLoS One 8 (2013), e77252.
[31] A. Kumar, M.D. Graham, Margination and segregation in confined flows of blood and other multicomponent suspensions, Soft Matter 8 (2012) 10536–10548.
[32] Z.J. Wu, P. Marascalco, J. Marhefka, M.V. Kameneva, Increased red blood cell deformation by minute concentrations of blood soluble dragreducing polymers (DRPs), Artif. Organs 49 (2003) 199.
[33] D.E. Bragin, S. Thomson, O. Bragina, G. Statom, M.V. Kameneva, E.M. Nemoto, Drag-reducing polymer enhances microvascular perfusion in the traumatized brain with intracranial hypertension, Acta Neurochir. 122 (2016) 25–29.
[34] K.L. Pitts, M. Fenech, Micro-particle image velocimetry for velocity profile measurements of micro blood flows, J. Vis. Exp. Jove (2013), e50314.
[35] E. Yeom, Y.J. Kang, S.J. Lee, Changes in velocity profile according to blood viscosity in a microchannel, Biomicrofluidics 8 (2014), 034110.
[36] P.K. Dagur, J.P. McCoy Jr., Collection, storage, and preparation of human blood cells, Curr. Protoc. Cytom. 73 (2015) 5.1.1–5.1.16.
[37] S. Fitzgibbon, A.P. Spann, Q.M. Qi, E.S.G. Shaqfeh, In vitro measurement of particle margination in the microchannel flow: effect of varying hematocrit, Biophys. J. 108 (2015) 2601–2608.
[38] H.L. Goldsmith, G.R. Cokelet, P. Gaehtgens, Robin Fahraeus: evolution of his concepts in cardiovascular physiology, Am. J. Physiol. 257 (1989) H1005–H1015.
[39] A.S. Popel, P.C. Johnson, Microcirculation and hemorheology, Annu. Rev. Fluid Mech. 37 (2005) 43–69.
[40] K. Namdee, A.J. Thompson, P. Charoenphol, O. Eniola-Adefeso, Margination propensity of vascular-targeted spheres from blood flow in a microfluidic model of human microvessels, Langmuir 29 (2013) 2530–2535.
[41] M. Cabel, H.J. Meiselman, A.S. Popel, P.C. Johnson, Contribution of red blood cell aggregation to venous vascular resistance in skeletal muscle, Am. J. Physiol. 272 (1997) H1020–H1032.
[42] G. Barshtein, D. Wajnblum, S. Yedgar, Kinetics of linear rouleaux formation studied by visual monitoring of red cell dynamic organization, Biophys. J. 78 (2000) 2470–2474.
[43] Y.F. Wu, P.S. Hsu, C.S. Tsai, P.C. Pan, Y.L. Chen, Significantly increased low shear rate viscosity, blood elastic modulus, and RBC aggregation in adults following cardiac surgery, Sci. Rep. 8 (2018) 7173.
[44] J. Dupire, M. Socol, A. Viallat, Full dynamics of a red blood cell in shear flow, Proc. Natl. Acad. Sci. USA 109 (2012) 20808–20813.
[45] C. Neto, D.R. Evans, E. Bonaccurso, H.J. Butt, V.S.J. Craig, Boundary slip in newtonian liquids: a review of experimental studies, Rep. Prog. Phys. 68 (2005) 2859–2897.
[46] R. Lima, S. Wada, S. Tanaka, M. Takeda, T. Ishikawa, K.I. Tsubota, Y. Imai, T. Yamaguchi, In vitro blood flow in a rectangular PDMS microchannel: experimental observations using a confocal micro-PIV system, Biomed. Microdevices 10 (2008) 153–167.
[47] R. Lima, S. Wada, S. Tanaka, M. Takeda, K. Tsubota, T. Ishikawa, T. Yamaguchi, Velocity measurements of blood flow in a rectangular PDMS microchannel assessed by confocal micro-PIV system, IFMBE Proc. 14 (2006) 283–286.
[48] K.L. Pitts, M. Fenech, An Analytic Study on the Effect of Alginate on the Velocity profiles of blood in rectangular microchannels using microparticle image velocimetry, PLoS One 8 (2013), e72909.
[49] R. Zhao, J.N. Marhefka, J.F. Antaki, M.V. Kameneva, Drag-reducing polymers diminish near-wall concentration of platelets in microchannel blood flow, Biorheology 47 (2010) 193–203.
[50] M.V. Kameneva, Z.J. Wu, A. Uraysh, B. Repko, K.N. Litwak, T.R. Billiar, M.P. Fink, R.L. Simmons, B.P. Griffith, H.S. Borovetz, Blood soluble drag-reducing polymers prevent lethality from hemorrhagic shock in acute animal experiments, Biorheology 41 (2004) 53–64.
[51] C. Liu, J. Guo, F. Tian, N. Yang, F. Yan, Y. Ding, J.Y. Wei, G. Hu, G. Nie, J.J.A. N. Sun, Field-free isolation of exosomes from extracellular vesicles by microfluidic viscoelastic flows, Am. Chem. Soc. Nano 11 (2017) 6968–6976.
[52] J.J. Bishop, P.R. Nance, A.S. Popel, M. Intaglietta, P.C. Johnson, Erythrocyte margination and sedimentation in skeletal muscle venules, Am. J. Physiol. Heart Circ. Physiol. 281 (2001) H951–H958.
[53] E.J. Lim, T.J. Ober, J.F. Edd, S.P. Desai, D. Neal, K.W. Bong, P.S. Doyle, G. H. McKinley, M. Toner, Inertio-elastic focusing of bioparticles in microchannels at high throughput, Nat. Commun. 5 (2014) 4120.
[54] A.M. Leshansky, A. Bransky, N. Korin, U.J.P.R.L. Dinnar, Tunable nonlinear viscoelastic “focusing” in a microfluidic device, Phys. Rev. Lett. 98 (2007), 234501.